A Novel Pulley-Based Simulator for Ureteroscopy with Visuo-Haptic Feedback

Jonathan Madera[1], Craig Peters[2], and Ann Majewicz Fey[1,2]

***Abstract*— This paper proposes a pulley-based haptic simulator device as training tool for ureteroscopy allowing for continuous insertion into a virtual ureter. The device motor provides a resistive feedback force to familiarize users with the forces experienced during surgery. We conducted a preliminary evaluation study with 7 subjects to compare subject performance using the system with visual and visuo-haptic feedback. Results support the utility of the device in terms of range forces rendered to the user and accurate following of the ureter profile. The addition of haptic feedback caused the subjects to perform the task more slowly. Future studies will evaluate if haptic feedback leads to enhanced skill development long-term with extended practice.**

I. INTRODUCTION

Ureteroscopy is the most common means to remove kidney or ureteral stones [1]–[4]. During ureteroscopy, several complications can arise, such as ureteral avulsion or perforation, due to the endoscopic diameter or excess applied force [5], [6]. Ureteral avulsion, a complete tear of the ureter, almost in-variably leads to major reconstructive surgery and possible loss of kidney function [7]–[11]. Ureteral perforation, a stretching of the ureter, is a more common adverse event. While perforation can be successfully managed with stent placement, there remains increased risk of ureteral stricture long-term. Experienced surgeons are able to minimize ureteral avulsions and perforations. However, novice surgeons unfamiliar with the proper range of insertion and extraction forces are more likely to cause damage. Proper preparation in the haptic experience of an ureteroscopic surgery would likely minimize devastating ureteral injuries.

Several surgical training models have been developed to help novice surgeons avoid complications when performing ureteroscopy [12], [13]. Inanimate models are inexpensive, but they lack the dynamic properties of a living system. Animal models are dynamic but costly, and variances with human organ systems in failure properties have limited use and effectiveness of these models [14], [15].

Virtual reality (VR) ureteroscopic surgery simulation devices have also been developed to provide novice surgeons with experience in urinary tract calculi removal. These systems have been shown to improve the performance of VR endoscopic tasks by novice endoscopists [16]–[18]. However, these systems do not incorporate haptic feedback - a critical modality to assess potential for tissue damage. Recently, a prototype has been developed to aid in reducing the risk of ureter wall perforation and avulsion by providing visual feedback of instantaneous extraction forces [19]. The prototype allows surgeons to see when they may be operating near a dangerous insertion/extraction force but distracts the surgeon from the workspace. There is still a need to train novice surgeons to understand the amount of force applied just before perforation or avulsion so that these accidents may be prevented in the future.

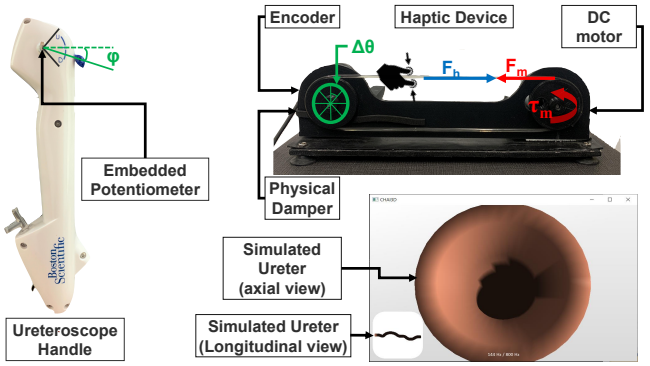

Fig. 1: Proposed haptic simulator for ureteroscopy consisting of a pulley-based haptic device, sensorized ureteroscope handle, and a custom virtual environment.

Virtual environments paired with haptic feedback have been shown to improve training for laparoscopic surgery and bone-sawing procedures [20]–[22]. Inspired by this work, we propose a prototype haptic simulation device that will lay the groundwork for creating a high fidelity VR simulation with realistic haptic feedback training tool for ureteroscopy. In this paper, we provide a description for the proposed device along with a preliminary investigation of user performance when using the device through a human subject study with 7 novice subjects. In a crossover experimental design, subjects performed simulated ureteroscopic insertion tasks with and without haptic feedback from the device, in a randomized order. We analyze a variety of performance metrics to determine potential benefits of haptic feedback for the simulator.

II. DEVICE DESIGN

The proposed haptic simulator for ureteroscopy has two degrees of freedom in sensing and one degree of freedom in haptic feedback. The device can be viewed as two integrated electro-mechanical subsystems, each providing one sensing

*This work was supported in part by the National Science Foundation Graduate Research Fellowship Program awarded to J. Madera

[1]J. Madera, A. M. Fey are with the Department of Mechanical Engineering at the University of Texas at Austin, Austin, TX 78712, USA {jonathan.madera,ann.majewiczfey}@utexas.edu

[2] C. Peters, A. M. Fey are faculty at the University of Texas Southwestern Medical Center Dallas, TX 75390, USA Craig.Peters@UTSouthwestern.edu

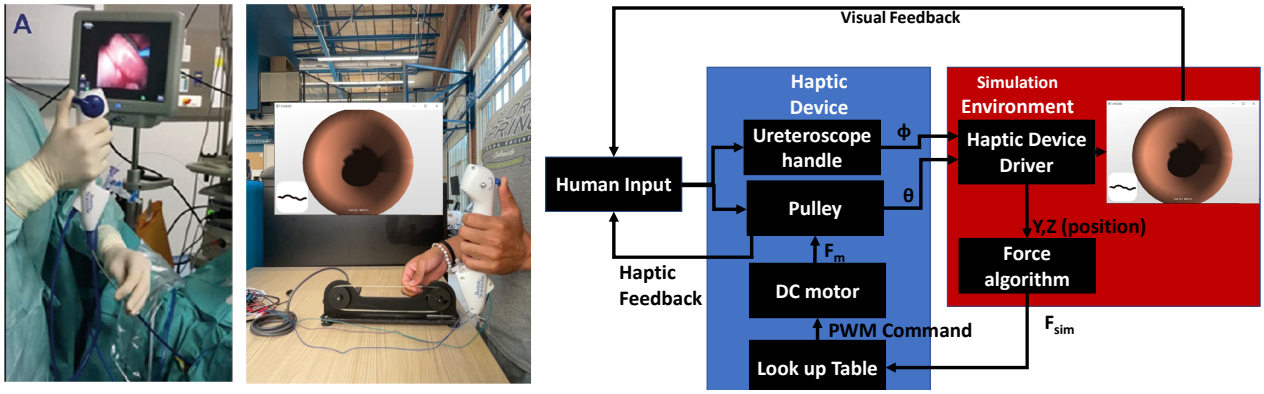

(a) Comparison of Ureteroscopic Simulator to Real Use Case

(b) Block Diagram of Simulator Operation

Fig. 2: Example of real ureteroscopic procedure (reproduced from [23]) shown with use of the proposed haptic simulator (a). Block diagram of human interaction with the haptic device and simulation environment (b).

degree of freedom for the ureteroscope tip. The two subsystems are integrated with CHAI3D, an open-source cross-platform C++ simulation framework for computer haptics and virtual reality [24]. The first subsystem is a mechanically driven pulley system that controls insertion for the simulated ureteroscope tip. The second subsystem is a modified handle of a Boston Scientific LithoVueTM Single Use Digital Flexible Ureteroscope that controls ureteroscope orientation. The Boston Scientific LithovueTM is a state of the art ureteroscope and is commonly used to perform ureteroscopy (Fig. 1, 2).

A. *Pulley System*

The pulley system consists of two 5 centimeter (2 inches) diameter pulleys placed roughly 25.4 centimeters (about 10 inches) apart and connected using a 3.175 millimeter (1/8-inch) diameter flexible round belt. The belt dimensions are modeled after the scope dimensions of the Boston Scientific LithoVueTM System. In comparison, the LithoVue System ureteroscope dimensions used in surgery contains a 2.6 millimeter (7.7F) tip diameter and a 3.2 millimeter (9.5F) outer sheath diameter [25]. It should be noted the belt diameter used in the proposed haptic training device closely matches the diameter of the outer sheath, as the sheath is what the surgeon maintains contact with throughout the surgery. The length of the apparatus was determined due to the typical length of the scope and the average length of a human ureter, approximately 25-30 centimeters [26]. This design allows for a simple display of the guided linear motion, the first physical degree of freedom, associated with the surgical procedure.

Attached to one pulley is a Nichibo 12V gearless DC motor (model 775-7013F-R/94). The motor supplies force feedback on the user by applying a torque, τ_m at the center of the pulley. The force felt by the user, supplied by the motor, F_m is the quotient of τ_m and the distance to the tangent of the pulley or its radius r_{pulley}. Users are provided feedback as they as they move the belt forwards or backwards using their fingertips, simulating the movement that is used by surgeons as they guide the scope through the ureter. The gearless

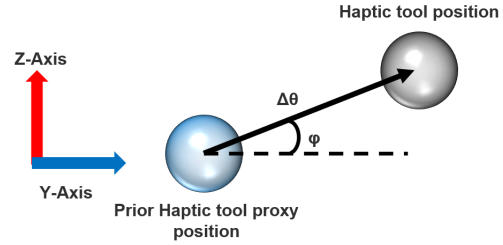

Fig. 3: Planar motion of the haptic proxy in the virtual environment, where $\Delta\theta$ relates the change in encoder ticks to absolute motion in one time step and ϕ, relates the ureteroscope handle position to the direction of motion.

functionality of the motor allows it to be back-drivable so users can operate back and forth in a linear motion. This motor is controlled using a Dual VNH5019 motor driver, external power supply, and an Arduino Uno. The other pulley is attached to a Yumo 1024 pulse per rotation incremental rotary encoder that is able to read the rotational position of the pulley as the belt moves. Using the data from the incremental rotary encoder the Arduino Uno transforms first physical degree of freedom into the linear motion in the virtual environment based on the encoder counts, θ (Fig. 3).

B. *Modified Boston Scientific LithoVueTM Handle*

The modified ureteroscope handle provides the second physical degree of freedom via an embedded potentiometer. It should be noted the handle is not physically connected to the pulley subsystem or any flexible ureteroscope. The potentiometer is actuated by the user in a similar fashion to the way a surgeon deflects the tip of the flexible ureteroscope by rotating the blue knob located at the top of the device. When the blue knob is rotated by the user, the potentiometer resistance value changes. The resistance value is read by the Arduino Uno and used to change the direction of linear motion in the virtual environment. The direction of motion is quantified as angle ϕ. In summary, the device has two

degrees of freedom and is capable of providing planar motion in the virtual environment (Fig. 3).

C. CHAI3D Virtual Environment

As the name suggests, CHAI3D (Computer Haptics Active Interface) is an open source set of libraries written in C++ developed for experimental haptics in the research community, capable of rendering forces to haptic devices in a three dimensional virtual world utilizing the OpenGL graphics platform. There are two objects in the custom built 3D virtual world environment used to simulate the forces felt during the ureteroscopy procedure, a haptic tool spherical point and a 3D simulated ureter solid object.

The haptic tool spherical point is used as a proxy for the ureteroscope. For higher fidelity, the haptic tool spherical point should be replaced with a deformable and flexible virtual ureteroscope object. However, due to the simplicity of the low cost proposed haptic device and the highly computationally expensive algorithm for mesh on mesh collisions, the ureteroscope is modeled as a spherical point and denotes the three dimensional cartesian coordinate position of the tip inside the virtual world. For clarity and continuity, it is worth restating how the haptic tool spherical position is interfaced by the human user. The human user can move the haptic point in a planar motion, two degrees of freedom, inside of the virtual environment by displacing the belt on the pulley subsystem to move linearly and turning the knob on the LithoVue handle to change the direction of the linear motion inside the virtual environment (Fig. 3). Equations (1) and (2) govern the transformation of the encoder position, θ, and ureteroscope knob angle, ϕ into the Cartestian coordinates, y and z, in the virtual world. As the device only allows for planar motion, the x position is kept constant. The subscript k denotes the time step. A scaling factor of 10240 is used to scale the high resolution encoder ticks.

$$y_{k+1} = y_k + \frac{\theta_k - \theta_{k-1}}{10240} \cos\phi \tag{1}$$

$$z_{k+1} = z_k + \frac{\theta_k - \theta_{k-1}}{10240} \sin\phi \tag{2}$$

The 3D simulated ureter solid object was created in SolidWorks as a uniformly cylindrical tube made of piecewise arc lengths. The center of the tube circle is placed at the center of the virtual world. The geometry of the simulated ureter object approximates human anatomy and it could easily be modified to use patient-specific data.

D. Force Rendering Algorithm

The main goal of this work was to design a device and simulation environment capable of demonstrating the forces typically associated in the ureteroscopy procedure. The rendered forces output by the device and felt by the human user should be consistent with what surgeons feel while performing an insertion or extraction from the ureter. While there are dynamic visco-elastic models for interaction forces of soft tissue deformation, many of them are infeasible as they require finite difference methods, which are known

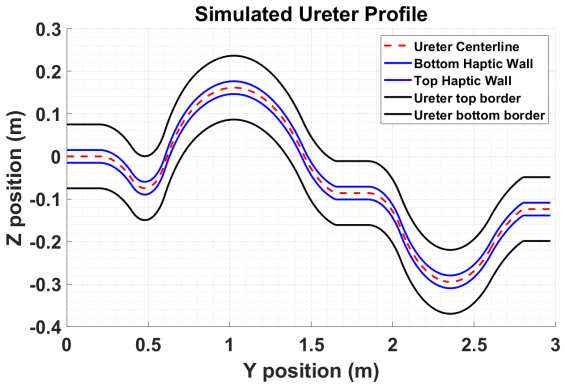

Fig. 4: Profile of simulated ureter and virtual haptic wall.

to be computationally expensive [27]. Other methods for soft body dynamics that do not require finite difference methods that have been used to render forces from soft body interactions fail in this particular setting because they rely on closed surface meshes [28]. A thin-walled tube geometry is a non-closed surface which makes deformable modeling a challenge. Therefore, we chose a simple yet versatile virtual wall model as a first approximation for rendering forces in the range of the ureteroscopy procedure. Additionally, the virtual wall model is a typical performance benchmark for haptic devices [29].

The virtual wall model employed in the human user studies and device validation is based on the center-line of the simulated ureter (Fig. 4). Two virtual walls are rendered at an offset distance, r_{iu}, from the of the ureteral center line. The ureter is aligned in the $y-z$ plane. For any given y value there is defined a $z_{desired}$, which corresponds to the ureteral center line. When the haptic tool position sufficiently crosses above or below the rendered virtual walls, the force increases proportionally to distance the tool is past the wall. A constant term β is added to the virtual wall to ensure the command to the motor is high enough to overcome the no load current rating of the motor. In order to keep the system passive, the force value is set to zero when the velocity of the haptic tool position, v, is less than or equal to 0. Passive is defined such that motor does not inject energy into the system causing the pulley to rotate in the opposite direction of user intention. This rendering force is shown below in Equation (3).

$$F_{sim} = \begin{cases} k\Delta z + \beta & z \geq z_{desired} + r_{iu}, \quad \text{given} \quad v \geq 0 \\ k\Delta z + \beta & z \leq z_{desired} - r_{iu}, \quad \text{given} \quad v \geq 0 \\ 0 & \text{Otherwise} \end{cases} \tag{3}$$

The force felt by the human user and output by the motor, F_m, is calculated based on the interaction force of the haptic tool with the ureteral wall, F_{sim}. Since the DC motor is controlled via Pulse Width Modulation (PWM) duty cycles, an experimentally based 1D Lookup table was constructed. To construct the Lookup table I, a constant duty cycle command was sent to the motor above an arbitrary encoder count, $\theta \geq 300$ counts. The experimenter held the pulley system above the set threshold and recorded the

current through the motor windings, i_{motor}, as measured by the motor driver for different values of duty cycle. Due to the noisy nature of recording i_{motor} and the characteristics of DC motors changing based on internal temperature, the process was conducted a total of five times for each duty cycle shown. The average values of i_{motor} were used for each duty cycle command. τ_m is directly proportional to i_{motor}, through the DC motor torque constant $k_{motor} = 0.0869 \frac{kgcm}{Amps}$, F_m was computed according to equation (4).

$$F_m = \frac{\tau_m}{r_{pulley}} \tag{4}$$

TABLE I: PWM, Current, Force Lookup Table

PWM	Avg i_{motor} (mA)	F_m (N)
30	2800	0.9545
40	5000	1.7044
50	6500	2.2157
60	8300	2.8293
70	9800	3.3406
80	11300	3.8519
90	13000	4.4314
120	18000	6.1358

III. USER STUDY

A. Experimental Protocol

In order to validate the proposed device as a surgical training tool, a human user study was conducted. Seven participants were recruited (mean age: 22, std age: 5). All partcipants were unveriisity affiliated. The protocol falls under the University of Texas at Austin IRB. Each human-user was first given a brief introduction on how to interface with the haptic device in the virtual environment. Once familiar with both the manipulation and the force feedback associated with collisions inside the ureteral wall, the subject was asked to complete six trials of the simulated task. For the purpose of this experiment, a trial consists of the human user navigating along the full length of the simulated ureter. The goal was to follow the path while avoiding the ureteral walls. For half of the trials, the subjects received haptic feedback, condition 'H', and for the other half of the trials no haptic feedback, condition 'NH', was provided. The order of conditions was randomized prior to the study.

B. Data Collection and Analysis

Data was collected at a frequency of 200 Hz. The timestamp of each data point, the haptic tool position, haptic tool velocity, ϕ, $z_{desired}$, F_{sim}, and i_{motor} was recorded to compute performance metrics. Note i_{motor} was equivalently equal to 0 during trials of 'NH'. The metrics computed were total time to complete the pass, the average error position error from z to $z_{desired}$ normalized over the trial time, the ratio of time when F_{sim} was rendered over total trial time, the ratio of time of a rendered force to the time when no force was rendered for each trial, the max force for each trial, and the average force over each trial normalized over time. All metrics were averaged for all trials and subjects with mean and standard deviations reported in Table II. All metrics except T_{total} were found to be normally distributed with homogenous variance according to the Jacque-Bera and Bartlett tests, respectively. Therefore, the 1D ANOVA statistical was used to compare significant difference between the two conditions, where $p-value \leq 0.05$ was considered significant. For T_{total}, the non-parametric Mann Whitney U test was used. To further investigate the validity of the proposed simulation paradigm, the recorded F_{sim} was separated into bins and the frequency of each force bin divided by the total number of force observations was plotted as a distribution for each condition. Lastly, the linear correlation between F_m and F_{sim} was computed for each trial in the 'H' condition.

C. Results

The outcome of the user study is shown below in Table II. Each metric is defined in order, top down, in Section III B. From Table II, it is shown there is little difference between the performance metrics in each condition 'H' vs 'NH'. The significantly different metric between conditions ($p = 0.0271$) was the total time to complete the trial. The 'H' condition took statistically significantly longer to complete than the 'NH' trial across subjects. Similarity between conditions is also shown in Fig. 5 where the distribution of forces is almost evenly split between the two conditions. The most frequent force bin observations were between 3N - 4N. In Fig. 6, an example plot of the correlation between F_m and F_{sim} is shown for one subject. In general, most observation pairs for each session are near the linear trend line. However, there are many outliers above and below the trendline indicating time points where there is a mismatch between the force output by the motor, F_m, and the computed force in simulation, F_{sim}.

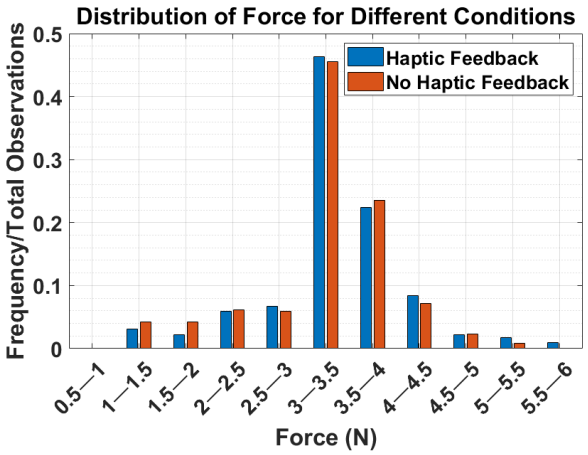

Fig. 5: Distribution of simulated force F_{sim} based on virtual wall rendering for all subjects in both the 'H' and 'NH' condition. Values are normalized on the total number of time points where F_{sim} is greater than 0.5N.

TABLE II: Performance Metrics: Means, standard deviation, and significant difference between conditions: T_{total} is the total time to complete the trial, Z_{error} is the average path error normalized by trial time, $\frac{T_{ff}}{T_{total}}$ is amount of time during a trial force was rendered over total trial time, $\frac{T_{ff}}{T_{nf}}$ is ratio of time force was rendered to amount of time with no force rendered, Avg Max F_{sim} is the computed max force averaged over trials, Avg F_{sim} is computed force averaged over trial time.

Metrics	Mean 'H'	Mean 'NH'	Std 'H'	Std 'NH'	P-val
T_{total} (s)	66.4340	40.8355	48.9683	14.6794	0.0157
Z_{error}	4.2956	4.3381	1.1238	1.0637	0.9005
$\frac{T_{ff}}{T_{total}}$	0.3163	0.2966	0.1035	0.1005	0.5357
$\frac{T_{ff}}{T_{nf}}$	0.4947	0.4483	0.2245	0.1967	0.4804
Avg Max F_{sim} (N)	4.3818	4.0934	0.9014	0.7982	0.2788
Avg F_{sim} (N)	0.9897	0.9264	0.3767	0.3562	0.5787

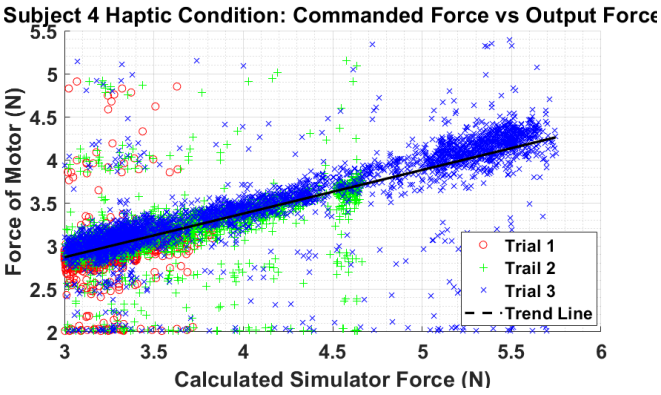

Fig. 6: Linear correlation of calculated simulator force, F_{sim} vs force of motor felt by human user, F_m at each time point for each trial. Deviations from the trend line indicate an instantaneous mismatch in the motor output and the calculated force in the virtual environment.

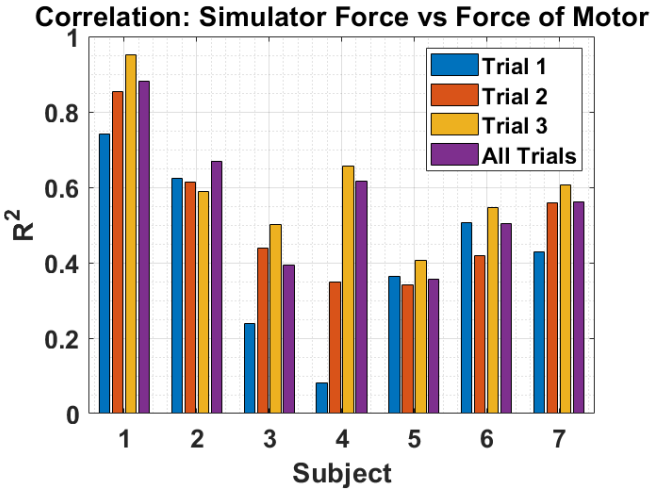

Fig. 7: Linear correlation coefficient, R^2 of calculated simulator force, F_{sim} vs force of motor felt by human user, F_m for individual trials and for all trials.

IV. DISCUSSION

Interestingly, the inclusion of haptic feedback for the task did not affect the task performance across many metrics. The most affected performance metric was the increase in T_{total}. The inclusion of haptic feedback likely forced the users to slow down and reconsider their trajectory. Additionally in the 'H' condition trials, users still receive feedback when correcting their trajectory as the haptic position needs to approach the center line of the ureter to proportionally decrease. It was hypothesized that the addition of haptic feedback would dramatically decrease the error in haptic position from the center as compared to no haptic feedback. Our results did not show statistically significant improvements in Z_{error} though the mean value was slightly lower. Subjects may have relied more on the visual feedback of the simulation to guide their trajectories, as compared to the haptic feedback. Other studies in haptics for motor learning have also shown ambivalent results on the addition of haptic guidance feedback for motor skill acquisition [30], [31]. Thus, it is possible the particular method of haptic rendering chosen for this study may be limited for enhancing performance. Future studies will include evaluating different forms of haptic feedback (e.g., varying haptic feedback gains or adding damping).

A positive result as shown by Fig. 5 is the forces rendered to the user indeed do match the forces typically seen in the ureteroscopy procedure as reported in literature by [15], [14], [32] to be between 0-6N with many of the forces in the middle, indicating little or no perforation and a low likelihood of ureteral avulsion. Despite this, one would expect the F_{sim} in the 'NH' condition to be distributed to higher value force bins and the opposite to occur in the 'H' condition. This emphasizes the idea that the subjects likely relied more on the visual than haptic feedback to complete the task. The R^2 correlation shown for each subject in Fig. 7, shows a discrepancy in the ability of the haptic device to provide the necessary force. Specifically, the relationship between F_m and F_{sim} should be linear, resulting in R^2 values near 1 for all trials. The scattering of data from the established linear trendline, shown in Fig. 6 suggest a potential issue with the device's ability to render stable forces. However, it is known that an otherwise stable haptic device can become unstable if the human user is not passive [29]. In Fig. 7,

most subjects' correlation increased from the first trial to the final third trial indicating improved performance with continued use. Furthermore, there is likely a time delay between the sent force command, F_{sim}, and the sampling of motor current, i_{motor}, especially during spikes of F_{sim} due to a sudden increase when the user momentarily halts inside of the virtual wall and then continues their motion.

V. CONCLUSIONS

Despite the lack of performance increases as a result of haptic feedback, the proposed simple pulley-based haptic device and simulation environment was able to render forces in the range typical of the ureteroscopy procedure to human users during the simulated task. User performance also seems to improve as a function of device use for most subjects. As a result, this work lays a preliminary foundation for the development of surgical training tool for ureteroscopy. An area of future work to further validate the proposed device and the virtual environment is to see how performance differs between novice users and expert surgeons, and to explore different types of haptic feedback or extended training practices that may enhance performance.

ACKNOWLEDGMENT

We would like to acknowledge the work of Adam Dunkels and his team for the protothread library.

REFERENCES

[1] J. Barnard, C. Crigger, A. Hajiran, O. Al-Omar, and M. Ost, "Pediatric Ureteroscopy," in *Ureteroscopy*. Springer, 2020, pp. 189–203.

[2] N. L. Miller and J. E. Lingeman, "Management of Kidney Stones," *BMJ*, vol. 334, no. 7591, pp. 468–472, 2007.

[3] G. Liguori, F. Antoniolli, C. Trombetta, M. Biasotto, A. Amodeo, G. Pomara, S. Bucci, and E. Belgrano, "Comparative Experimental Evaluation of Guidewire Use in Urology," *Urology*, vol. 72, no. 2, pp. 286–289, 2008.

[4] N. Patel and M. Monga, "Ureteral Access Sheaths: A Comprehensive Comparison of Physical and Mechanical Properties," *International Brazilian Journal of Urology : official journal of the Brazilian Society of Urology*, vol. 44, no. 3, pp. 524–535, 2018.

[5] "Studies from Southern Illinois University Yield New Data on Urology (Significance of Extraction Forces in Kidney Stone Basketing)," 2015.

[6] Z. Najafi, *Development of New Treatment Modalities for Kidney/Ureter Stones*. The University of Akron, 2015.

[7] T. Flam, M. Malone, and R. Roth, "Complications of Ureteroscopy," *The Urologic clinics of North America*, vol. 15, no. 2, p. 167—181, May 1988.

[8] "Complications of Urinary Stone Surgery," in *Urinary Stone Disease*, ser. Current Clinical Urology. Totowa, NJ: Humana Press, 2007, pp. 511–553.

[9] A. Gaizauskas, M. Markevicius, S. Gaizauskas, and A. Zelvys, "Possible Complications of Ureteroscopy in Modern Endourological Era: Two-Point or "Scabbard" Avulsion," *Case reports in urology*, vol. 2014, pp. 308 093–6, 2014.

[10] P.-J. Tsai, H.-Y. J. Wang, T.-B. Chao, and C.-C. Su, "Management of Complete Ureteral Avulsion in Ureteroscopy," *Urological Science*, vol. 25, no. 4, pp. 161–163, 2014.

[11] F. F. Önol, Y. Tanỳdỳr, A. Akba, E. Özbek, and . Önol, "Management of Ureteral Avulsion as a Complication of Ureterorenoscopy," *Turk J Urol*, vol. 35, pp. 185–90, 2009.

[12] M. Brehmer and D. A. Tolley, "Validation of a Bench Model for Endoscopic Surgery in the Upper Urinary Tract," *European Urology*, vol. 42, no. 2, pp. 175–180, 2002.

[13] O. Brunckhorst, A. Aydin, H. Abboudi, M. Khan, P. Dasgupta, and K. Ahmed, "Ureteroscopy Simulation - A Systematic Review of Current Training Modalities," *Journal of Urology, The*, vol. 191, no. 4, pp. e872–e872, 2014.

[14] D. P. Sokolis, "In Vitro Study of Age-Related Changes in Human Ureteral Failure Properties According to Region, Direction, and Layer," *Proceedings of the Institution of Mechanical Engineers. Part H, Journal of engineering in medicine*, vol. 233, no. 5, pp. 570–583, 2019.

[15] R. N. Pedro, K. Hendlin, D. Weiland, A. Ramani, T. S. Köhler, J. K. Anderson, and M. Monga, "In Vitro Evaluation of Ureteral Perforation Forces," *Urology*, vol. 70, no. 3, pp. 592–594, 2007.

[16] K. Ogan, L. Jacomides, M. J. Shulman, C. G. Roehrborn, J. A. Cadeddu, and M. S. Pearle, "Virtual Ureteroscopy Predicts Ureteroscopic Proficiency of Medical Students on a Cadaver," *The Journal of urology*, vol. 172, no. 2, pp. 667–671, 2004.

[17] D. M. Wilhelm, K. Ogan, C. G. Roehrborn, J. A. Cadeddu, and M. S. Pearle, "Assessment of Basic Endoscopic Performance Using a Virtual Reality Simulator," *Journal of the American College of Surgeons*, vol. 195, no. 5, pp. 675–681, 2002.

[18] E. D. Matsumoto, K. T. Pace, and R. J. D'A HONEY, "Virtual Reality Ureteroscopy Simulator as a Valid Tool for Assessing Endourological Skills," *International journal of urology*, vol. 13, no. 7, pp. 896–901, 2006.

[19] Z. Najafi, T. Tieu, A. M. Mahajan, and B. F. Schwartz, "Design of a New Stone Extraction Device with Force Feedback," *International Journal of Biomedical Engineering and Technology*, vol. 20, no. 2, pp. 166–178, 2016.

[20] T. R. Coles, D. Meglan, and N. W. John, "The Role of Haptics in Medical Training Simulators: A Survey of the State of the Art," *IEEE transactions on haptics*, vol. 4, no. 1, pp. 51–66, 2011.

[21] Y. Lin, X. Wang, F. Wu, X. Chen, C. Wang, and G. Shen, "Development and Validation of a Surgical Training Simulator with Haptic Feedback for Learning Bone-Sawing Skill," *Journal of Biomedical Informatics*, vol. 48, pp. 122–129, 2014.

[22] O. A. J. van der Meijden and M. P. Schijven, "The Value of Haptic Feedback in Conventional and Robot-Assisted Minimal Invasive Surgery and Virtual Reality Training: A Current Review," *Surgical endoscopy*, vol. 23, no. 6, pp. 1180–1190, 2009.

[23] S. Butticè, T. E. Şener, C. Netsch, E. Emiliani, R. Pappalardo, and C. Magno, "LithoVue^{TM}: A new single-use digital flexible ureteroscope," *Central European Journal of Urology*, vol. 69, pp. 302 – 305, 2016.

[24] F. Conti, F. Barbagli, D. Morris, and C. Sewell, "Chai 3d: An Open-Source Library for the Rapid Development of Haptic Scenes," *IEEE World Haptics*, vol. 38, no. 1, pp. 21–29, 2005.

[25] B. Winship and M. Lipkin, "Single-Use Flexible Ureteroscopes," in *Ureteroscopy*. Springer, 2020, pp. 73–83.

[26] G. Faerber, A. H. Lebastchi, and R. P. Jen, "Ureteral Anatomy," *Smith's Textbook of Endourology*, pp. 453–464, 2019.

[27] X. P. Liu, S. Xu, H. Zhang, and L. Hu, "A New Hybrid Soft Tissue Model for Visio-Haptic Simulation," *IEEE Transactions on Instrumentation and Measurement*, vol. 60, no. 11, pp. 3570–3581, 2011.

[28] J. Berkley, G. Turkiyyah, D. Berg, M. Ganter, and S. Weghorst, "Real-Time Finite Element Modeling for Surgery Simulation: An Application to Virtual Suturing," *IEEE Transactions on visualization and computer graphics*, vol. 10, no. 3, pp. 314–325, 2004.

[29] D. W. Weir and J. E. Colgate, "Stability of Haptic Displays," *Haptic Rendering: Foundations, Algorithms, and Applications*, pp. 123–156, 2008.

[30] J. Liu, S. Cramer, and D. Reinkensmeyer, "Learning to Perform a New Movement with Robotic Assistance: Comparison of Haptic Guidance and Visual Demonstration," *Journal of neuroengineering and rehabilitation*, vol. 3, no. 1, pp. 1–10, 2006.

[31] L. Marchal-Crespo, M. van Raai, G. Rauter, P. Wolf, and R. Riener, "The Effect of Haptic Guidance and Visual Feedback on Learning a Complex Tennis Task," *Experimental brain research*, vol. 231, no. 3, pp. 277–291, 2013.

[32] S. Tapiero, K. S. Kaler, P. Jiang, S. Lu, C. Cottone, R. M. Patel, Z. Okhunov, M. J. Klopfer, J. Landman, and R. V. Clayman, "Determining the Safety Threshold for the Passage of a Ureteral Access Sheath in Clinical Practice Using a Purpose-Built Force Sensor," *The Journal of Urology*, pp. 10–1097, 2021.